HHS Public Access

Author manuscript

Metabolism. Author manuscript; available in PMC 2017 January 01.

Published in final edited form as:

Metabolism. 2016 January ; 65(1): 26–35. doi:10.1016/j.metabol.2015.09.012.

Autocrine Effect of Vascular Endothelial Growth Factor-A is Essential for Mitochondrial Function in Brown Adipocytes

Kiana Mahdaviani[1], **David Chess**[1], **Yuanyuan Wu**[1], **Orian Shirihai**[1], and **Tamar Aprahamian**[2]

[1]Section of Endocrinology, Department of Medicine, Boston University School of Medicine, Boston, MA 02118, USA

[2]Renal Section, Department of Medicine, Boston University School of Medicine, Boston, MA 02118, USA

Abstract

Objective—The obesity epidemic in the United States, and the accompanying condition of type 2 diabetes, puts a majority of the population at an increased risk of developing cardiovascular diseases including coronary artery disease, stroke, and myocardial infarction. In contrast to white adipose tissue (WAT), brown adipose tissue (BAT), is well vascularized, rich in mitochondria, and highly oxidative. While it is known that the angiogenic factor VEGF-A is required for brown adipocyte development, the functional consequences and exact mechanism remain to be elucidated. Here, we show that VEGF-A plays an essential autocrine role in the function of BAT.

Materials and Methods—Mouse models were generated with an adipose-specific and macrophage-specific ablation of VEGF-A. Adipose tissue characteristics and thermogenic response was analyzed *in vivo,* and mitochondrial morphology and oxidative respiration was analyzed *in vitro* to assess effects of endogenous VEGF-A ablation.

Results—VEGF-A expression levels are highest in adipocyte precursors compared to immune or endothelial cell populations within both WAT and BAT. Loss of VEGF-A in adipocytes, but not macrophages, results in decreased adipose tissue vascularization, with remarkably diminished thermogenic capacity *in vivo*. Complete ablation of endogenous VEGF-A decreases oxidative capacity of mitochondria in brown adipocytes. Further, acute ablation of VEGF-A in brown adipocytes *in vitro* impairs mitochondrial respiration, despite similar mitochondrial mass compared to controls.

Conclusion—These data demonstrate that VEGF-A serves to orchestrate the acquisition of thermogenic capacity of brown adipocytes through mitochondrial function in conjunction with the recruitment of blood vessels.

Send correspondence to: Tamar R. Aprahamian, Ph.D., Boston University School of Medicine, Department of Medicine-Renal Section, 650 Albany Street, 5th floor, Boston, MA 02118, Phone: +1 617 414 3368, Fax: +1 617 638 7326, aprahami@bu.edu.

Disclosure. The authors declare no conflict of interest.

Keywords

Adipocyte; adipose tissue; mouse; mitochondria; vascular endothelial growth factor (VEGF)

1. Introduction

The obesity epidemic in the United States, and the accompanying condition of diabetes, puts a large portion of the population at increased risk of developing cardiovascular complications. A new report predicts that half of the United States population will be obese by 2030. An area of recent research interest is the status of adipose tissue vascularity. It has been shown that obese mice display capillary rarefaction in white adipose tissue (WAT) and reductions in the expression of the angiogenic growth factor VEGF-A, which correlates with the appearance of hypoxia and impaired glucose tolerance (1-4).

The study of brown adipose tissue (BAT) has recently become an area of intense investigation. The presence of active BAT in human adults has recently been confirmed (5) and the amount of BAT is negatively correlated with obesity and age (6). High expression of VEGF-B is present in BAT, where it facilitates fatty acid uptake by endothelial cells (7). In mice, cold exposure has been shown to induce VEGF expression in BAT, leading to increased vessel permeability, which facilitates triglyceride clearance (8,9). While angiogenesis has been demonstrated to be an essential component in BAT development, how this is orchestrated or synchronized with the development and ability of the tissue to consume oxygen and fuel from circulation has not been determined. Taken together, the detailed examination of angiogenesis in BAT is warranted as it may provide novel targets to modulate obesity and associated cardiovascular complications.

Although adipose tissue dysfunction and capillary rarefaction are known to occur in obesity and are presumed to be detrimental to metabolism, studies dissecting the molecular targets involved in the ensuing metabolic dysfunction are lacking. It has been demonstrated that prolonged exposure to cold leads to increased BAT angiogenesis, independent of hypoxia (10). This was associated with the induction of VEGF-A; however, conflicting results were obtained with different VEGF inhibitors (neutralizing antibodies targeting the receptors, VEGFR1 and VEGFR2). Because the angiogenesis regulatory network is complex, and VEGFR1 and VEGFR2 interact with multiple ligands (VEGF-A, VEGF-B, VEGF-C, VEGF-D (encoded by different genes), PIGF, and others), the molecular identities of the angiogenic factors regulating BAT and thermogenesis remain unknown.

A recent study has shown expression of VEGF isoforms and receptors in developing BAT and demonstrated that VEGF is necessary for survival and proliferation of brown adipocytes (11), however the functional consequences and mechanism of action of VEGF ablation were not studied in detail. It has also been shown that VEGF has autocrine effects on cells in the retina, kidney, and mammary gland (12-14); however, the functional consequences of VEGF-A in brown adipocytes remain to be elucidated. Here, we address the role of endogenous VEGF-A in BAT by utilizing our mouse model with adipose-specific VEGF-A ablation. Our results suggest that VEGF-A acts in an autocrine manner to facilitate the

thermogenic response and to promote brown adipocyte function through regulation of mitochondria.

2. Materials and Methods

2.1 Isolation of stromal vascular cells (SVC) and fluorescence activated cell sorting (FACS)

Inguinal and gonadal fat pads, as well as the interscapular BAT depot, were excised and primary adipocytes and SVCs were isolated as previously described (15). SVCs were resuspended in ice cold flow cytometry staining buffer (eBioscience Inc., San Diego, CA) supplemented with Fc block: purified anti-mouse CD16/32 antibody at 10 μg/ml. The cell suspension was incubated with antibodies for 90 min on ice, followed by washing with ice cold PBS and then 5 min DAPI (4′,6-diamidino-2-phenylindole) staining. Cells were resuspended in flow cytometry staining buffer and sorted on Moflo™ Legacy cell sorter (Beckman coulter Inc., Brea, CA). The isolation strategy was based on Rodeheffer et al. (16), with some modifications. First, based on FSC (Forward Scatter) and SSC (Side Scatter), single cells were selected. Second, dead cells were excluded based on their uptake of DAPI. Third, live singlets were further separated based on cell surface markers. Antibodies were purchased from eBioscience (CD45-FITC, CD31-FITC, Ter119-FITC, Sca-1-PE, CD34-Alexa700 and purified Fc block: CD16/32) and Biolegend (CD29-PE/cy5, San Diego, CA).

2.2 Mouse models and tissue collection

Fabp4-cre and LysM-cre were purchased from Jackson Laboratories (#005069 and #004781, respectively). Fabp4-cre transgenic and $VEGF^{flox/flox}$ mice (provided by Genentech) were used in a series of crosses to create mice ± cre and homozygous for flox, thereby ablating VEGF-A in adipose tissue. Similarly, LysM-cre transgenic and $VEGF^{flox/flox}$ mice were used in a series of crosses to create mice ± cre and homozygous for flox, thereby ablating VEGF in macrophages. The epididymal fat pad (WAT) and intrascapular BAT were collected, weighed, and subsequently divided in order to provide uniform tissue samples for further analyses. Heart and lung tissue were also collected for protein analysis. All experiments were approved by the Institutional Animal Care and Use Committee at Boston University.

2.3 Capillary density

To visualize the vasculature in WAT and BAT of Fabp4cre(+).$VEGF^{flox/flox}$ and control mice, 100 μl of the fluorescein isolectin Griffonia simplicifolia (Vector Labs) was administered to the circulation via cardiac injection 5 min. before sacrifice. Live, non-fixed adipose tissue specimens from WAT and BAT were minced and incubated with BODIPY for 1 hr to visualize adipocytes (17). Confocal microscopy was used to determine capillary density on 50-μm thick tissue stacks. Quantification of capillary density was assessed by measurement of lectin (FITC) luminosity on 10 randomly selected photomicrographs from each mouse sample.

2.4 Semi-quantitative PCR

A portion of the WAT and BAT tissue was snap frozen in liquid nitrogen immediately after harvest. Tissue was disrupted using a Qiagen TissueLyser, followed by total RNA extraction using the Qiagen RNeasy Kit (Valencia, CA). cDNA was produced using ThermoScript RT-PCR Systems (Invitrogen, Carlsbad, CA). VEGF, Ucp1, and Dio2 transcript was analyzed using Taqman Gene Expression Assays: #Mm01281449; Mm01244861_m1, and Mm00515664_m1, respectively (Applied Biosystems). Transcript levels were determined relative to the signal from GAPDH (Taqman Gene Expression Assay, #Mm99999915_m1) and normalized to the mean value of samples from control mice.

2.5 VEGF-A Protein Quantification

Tissue and cell samples were collected and subjected to homogenization by TissueLyser (Qiagen) and protein extraction. Levels of VEGF-A protein were determined using a mouse VEGF-A ELISA kit according to the manufacturer's instructions (R&D systems).

2.6 Acute Cold Exposure

Subcutaneous, biocompatible, and sterile microchip transponders (Bio Medic Data Systems, Seaford, DE) were implanted in male Fabp4cre(+).VEGF$^{flox/flox}$, Fabp4cre(−).VEGF$^{flox/flox}$, LysMcre(+).VEGF$^{flox/flox}$, and LysMcre(−).VEGF$^{flox/flox}$ mice at least two days prior to experimentation. On the day of the experiment, mice were housed singly in pre-chilled cages at 4°C with free access to water. Body temperature was assessed hourly for 6 or 24 hours using a wireless reader system (Bio Medic Data Systems, Seaford, DE).

2.7 Immunostaining

Slides of formalin-fixed BAT containing 5μm paraffin embedded sections from Fabp4cre(+).VEGF$^{flox/flox}$ and Fabp4cre(−).VEGF$^{flox/flox}$ mice were deparaffinized, stained with Tomm20 by immunofluorescence and immunohistochemistry, and imaged as previously described (18).

2.8 Cell culture and oxygen consumption measurements

Brown adipocytes were differentiated from mice and cultured as previously described in detail (19). Briefly, BAT from 4 week old male Fabp4cre(+).VEGF$^{flox/flox}$ and Fabp4cre(−).VEGF$^{flox/flox}$ mice was resuspended in 6 ml ofculture medium after collagenase digestion and washing steps. For oxygen consumptionexperiments, 100 μl were seeded into each well of a V7 cell culture plate (Seahorse Bioscience,Billerica, MA), followed by cell attachment for 1 h and addition of 150 μl medium consisting of DMEM supplemented with 10% fetal calf serum, 60 nM insulin, 10 mM HEPES, 4 mM glutamine, 50 IU of penicillin, 50 μg streptomycin, 25 μg sodium ascorbate/mL and 1 μM rosiglitazone. Medium was changed the day after seeding and thereafter every second day until pre-adipocytes had differentiated into brown adipocytes after 7 days of culture. Rosiglitazone (Toronto Research Chemicals, Ontario, Canada) was used as differentiation agent (20). For oxygen consumption measurements, brown adipocytes were switched to assay media (3 mM glucose, 0.8 mM Mg^{2+}, 1.8 mM Ca^{2+}, 143 mM NaCl, 5.4 mM KCl, 0.91 mM NaH_2PO_4, and Phenol red 15 mg/ml (Seahorse Bioscience), followed by incubation for 60 min. at 37

°C (no CO_2) before loading into the XF24 respirometry machine (Seahorse Bioscience) (21). During this time, a cartridge with the injection compounds (50 μl/port) used during the experiment was prepared and the machine was programmed. Stimulated energy expenditure is reported as the increase in oxygen consumption rate (OCR) in response to 1 μM norepinephrine (NE), and maximal respiratory capacity is determined as the maximal OCR and tested in the presence of the uncoupler, FCCP (5 μM) and 10mM sodium pyruvate. Values presented were normalized to OCR values after antimycin treatment which shows non-mitochondrial respiration. In experiments utilizing adenovirus, brown adipocytes isolated from Fabp4cre(−).$VEGF^{flox/flox}$ mice were treated on day 4 of differentiation with either Adeno-Cre-GFP or Adeno-GFP (Vector Biolabs, Philadelphia, PA) with a multiplicity of infection of approximately 1500. Experiments were run in triplicate and data were combined in order to perform statistics.

2.9 Western blotting

Protein extracts were subjected to SDS–polyacrylamide gel electrophoresis and immunoblotting using the following primary antibodies: VEGF (Santa Cruz (sc-152), UCP-1 (Abcam), and porin (Abcam).

2.10 Statistical Analysis

Differences between mean values were assessed by a students t-test; a p-value < 0.05 was considered significant.

3. Results

3.1 Expression of VEGF-A in adipocyte precursor cells

Adipose tissue contains cell populations within the stromal vascular fraction that have distinct gene expression signatures, including those for hematopoietic stem cells, endothelial cells, and adipocyte precursor cells (16). In order to define the cell populations producing the highest levels of VEGF-A, subcutaneous and gonadal WAT was dissected and the stromal vascular cells were isolated and sorted according to the aforementioned signatures. RNA expression analysis of the sorted cell populations revealed that the vast majority of VEGF-A in adipose tissue is derived from the adipocyte precursor fraction ($CD45^-$ $CD31^-$ $Ter119^-$ $CD34^+$ $SCA1^+$) (Fig. 1). We performed a similar analysis on these cell populations sorted from BAT, which revealed that the level of VEGF-A was also significantly higher in the population of adipocyte precursors within BAT, and also in comparison to WAT (Fig. 1). These results are the first to report that the adipocyte precursor population expresses the highest amounts of VEGF-A compared to the hematopoietic stem cell or endothelial cell populations ($CD45^+$ $CD31^+$ $Ter119^+$ $CD34^-$ $SCA1^-$) and that expression is significantly higher in this population from BAT versus WAT. These results suggest that VEGF-A plays a greater role in BAT function compared to WAT, and that expression in brown adipocytes could be essential to both expansion and function of the adipose tissue.

3.2 Generation of tissue-specific VEGF-A deficient mice

Based on our findings that adipocyte-derived VEGF-A is highly expressed compared to other cell types within adipose tissue, we generated mice with a VEGF-A-specific ablation

in adipocytes. We utilized Fabp4-cre transgenic and VEGF$^{flox/flox}$ mice in a series of crosses to create our experimental Fabp4cre(−).VEGF$^{flox/flox}$ and Fabp4cre(+).VEGF$^{flox/flox}$ mice.

We acknowledge that there is controversy regarding the specificity of the Fabp4-cre promoter as a model for ablation in adipose tissue; however, Fabp4-cre has been reasonably well-characterized in previous studies targeting adipose tissue (22-29). To exclude the possibility that any observed effects might be due in part to a macrophage response to reduced VEGF-A expression, we also targeted the monocyte/macrophage leukocyte lineage. We used the LysM-cre transgenic mouse to generate a macrophage-specific deletion of VEGF-A, the LysMcre.VEGF$^{flox/flox}$ mouse model. Two previous independent publications ablating VEGF in macrophages via cre-lox techonology did not report results on functional consequences to vascularization or thermogenesis (30,31).

We observed at least a 50% reduction in VEGF-A protein levels in whole WAT and BAT from Fabp4cre(+).VEGF$^{flox/flox}$ (Fig. 2a), but not in LysMcre(+).VEGF$^{flox/flox}$ mice, in which only macrophage expression of VEGF-A was decreased (Fig. 2d). Importantly, VEGF-A levels remained unchanged in macrophages of Fabp4cre(+).VEGF$^{flox/flox}$ compared to Fabp4cre(−).VEGF$^{flox/flox}$ (Fig. 2a). VEGF-A levels in heart and lung were similar to those previously reported and did not change regardless of cre expression (Fig. 2b). In adipocytes and SVF isolated from BAT, we observe diminished expression of VEGF-A to a greater extent in adipocytes from Fabp4cre(+).VEGF$^{flox/flox}$ mice compared to controls (Fig. 2c). Decreased adipose tissue expression of VEGF-A did not change body weight (Fig. S1) or total WAT weight in young Fabp4cre(+).VEGF$^{flox/flox}$ mice (Fig. 2f). In contrast to WAT, BAT weight was significantly decreased in Fabp4cre(+).VEGF$^{flox/flox}$ compared to Fabp4cre(−).VEGF$^{flox/flox}$ mice (Fig. 2f). The percentage of white adipose tissue to total body weight is 1.6 and 1.7 for Fabp4cre(−).VEGF$^{flox/flox}$ and Fabp4cre(+).VEGF$^{flox/flox}$ mice, respectively. The percentage of brown adipose tissue to total body weight is 0.26 and 0.15 for Fabp4cre(−).VEGF$^{flox/flox}$ and Fabp4cre(+).VEGF$^{flox/flox}$ mice, respectively. Therefore, we can confidently conclude that the absence of VEGF-A decreases brown adipose tissue weight significantly, and this is not due to changes in total body weight. In comparison, neither WAT nor BAT weight was affected by deletion of VEGF-A in macrophages (Fig. 2e).

Although WAT weight was unchanged, similar to a recent report (4), adipose-specific VEGF-A deficiency resulted in decreased WAT vascularity in Fabp4cre(+).VEGF$^{flox/flox}$ mice (Fig. 2g). Quantitative analysis revealed a statistically significant decrease in adipose tissue vascularity of Fabp4cre(+).VEGF$^{flox/flox}$ compared to LysMcre(−).VEGF$^{flox/flox}$, or LysMcre(+).VEGF$^{flox/flox}$ mice (Fig. 2h, and Fig. S2).

3.3 VEGF-A controls vascularity and function in brown adipose tissue

Our observation of decreased BAT weight was striking; therefore, we also assessed the extent to which the deficiency of VEGF-A affected the molecular markers of brown adipocytes. Examination of UCP1 and Dio2 mRNA expression levels revealed a decrease in Fabp4cre(+).VEGF$^{flox/flox}$ (Fig. 3a-b) compared to control mice. In addition, and similar to that observed in WAT, there was a significant decrease in BAT vascularity (Fig. 3c). Quantitative analysis revealed a statistically significant decrease in adipose tissue

vascularity of Fabp4cre(+).VEGF$^{flox/flox}$ mice compared to Fabp4cre(−).VEGF$^{flox/flox}$ mice (Fig. 3d). In control mice, we demonstrate that VEGF-A levels are higher in BAT compared to WAT (Fig. 1), suggesting that correspondingly more blood vessels would be a reasonable observation. Histological analysis of BAT by hematoxylin and eosin staining reveals striking morphological abnormalities when VEGF-A is ablated with regard to lipid droplet enlargement and coalescence (Fig. 3e). Ablation of VEGFA in macrophages was inconsequential to BAT marker expression, vascularity, and lipid architecture when compared to control mice (Fig. S2).

To test if the observed histological and vascular abnormalities in the Fabp4cre(+).VEGF$^{flox/flox}$ mice had functional consequences, we studied the effect of VEGF-A deletion on thermogenesis under cold exposure in young mice. The results revealed a dramatically impaired thermogenic response in Fabp4cre(+).VEGF$^{flox/flox}$ compared to Fabp4cre(−).VEGF$^{flox/flox}$ mice (Fig. 4a) over the six-hour time course. In contrast to the adipose-specific VEGF-A deletion, lack of VEGF-A in macrophages did not have any effect on thermogenic response to cold, even when the time course was extended to 24h observations (Fig. 4b). This corroborates our results in sorted adipose-derived stromal vascular fraction populations (Fig. 1), suggesting that the major role of VEGF-A in the adipose tissue occurs from the adipocyte population. Therefore, VEGF-A expression in the adipocyte population is instrumental not only to BAT vascularization, but also to BAT function. Taken together, these results suggest an autocrine effect of VEGF-A on brown adipocytes and an essential role in thermogenesis.

3.4 Impaired thermogenic capacity of VEGF-A-deficient brown adipocytes

To determine if abnormal or dysfunctional mitochondria within the brown adipocytes were responsible for the decreased thermogenic response, we examined the BAT of Fabp4cre(+).VEGF$^{flox/flox}$ and Fabp4cre(−).VEGF$^{flox/flox}$ mice by confocal microscopy. Histological staining with Tomm20, an outer mitochondrial membrane protein, shows that BAT from Fabp4cre(+).VEGF$^{flox/flox}$ mice has decreased mitochondrial mass and exhibits signs of mitochondrial fragmentation, defined as being small, with abnormal structure (Fig. 5a). In contrast, BAT from Fabp4cre(−).VEGF$^{flox/flox}$ contains more mitochondria exhibiting a ring-shaped structure (arrows, Fig. 5a), which is a sign of normal NE stimulation as previously reported (18). These data suggest that mitochondrial abnormalities in the Fabp4cre(+).VEGF$^{flox/flox}$ BAT could be due to the lack of NE signaling or inability of the mitochondria to properly change their morphology in response to the NE signaling.

In order to provide further evidence that our observed effects were not due to VEGF-A secretion by other cells and to confirm autocrine behavior of VEGF-A on BAT independent of vascularization or hypoxia, we assessed the bioenergetic capacity of VEGF-A-deficient brown adipocytes. The effect of VEGF-A deletion in mature cells was studied *in vitro* using isolated brown adipocytes from Fabp4cre(−).VEGF$^{flox/flox}$ and Fabp4cre(+).VEGF$^{flox/flox}$ mice. On day 8, protein expression levels of VEGF-A, UCP-1, and porin (known to decrease with reduced mitochondrial mass) were measured in the cells and significantly decreased in the adipocytes lacking VEGF-A (Fig. 5b-c). Stimulated energy expenditure was defined and calculated as the stimulus-induced fold increase in absolute oxygen consumption rates

(OCR, pmols O_2/min) over the pre-stimulus value. Both pre- and post- stimuli OCR values take into account the post-antimycin OCR value as a reference point (zero). We demonstrate here that the OCR of VEGFA-deficient brown adipocytes significantly decreased compared to control brown adipocytes (Fig. 5d-f). Thus, complete ablation of VEGF-A from brown adipocytes results in structural mitochondrial abnormalities and decreased capacity for mitochondrial respiration.

3.5 Distinct effects on differentiation of brown adipocytes after acute ablation of VEGF-A

To determine the acute effect of VEGF-A deletion, and in order to exclude the potential effect on differentiation, we treated $VEGF^{flox/flox}$ brown adipocytes *in vitro* on day 4 with an adenovirus encoding either cre-recombinase (Ad-Cre) or control (Ad-CMV). On day 8, determination of VEGF-A and UCP-1 protein levels in the brown adipocyte cultures revealed significant decreases in $VEGF^{flox/flox}$ brown adipocytes treated with Ad-Cre compared to Ad-CMV (Fig. 6a). However, expression of porin, known to decrease with reduced mitochondrial mass, did not change. At this time, there were also no differences in size or number of lipid droplets between the groups (Fig. S3). A similar trend to the effect observed in brown adipocytes isolated from adipose-specific VEGF-A-deficient mice. Mitochondrial respiration of $VEGF^{flox/flox}$ brown adipocytes treated with Ad-Cre did not affect mitochondrial maximal oxidative capacity which is examined by FCCP. However, mitochondrial respiration was significantly impaired in response to NE even with short term VEGF deficiency (Fig. 6b-d). This indicates that acute ablation of VEGF-A during differentiation is sufficient to impair mitochondrial function, while maintaining organellar mass and structural integrity.

Taken together, these *in vitro* studies use both genetically modified mice and adenoviral treatment to demonstrate that VEGF-A ablation in brown adipocytes decreases the oxidative capacity of these cells. Therefore, VEGF-A from brown adipocytes provides autocrine signaling which facilitates mitochondrial oxidative and thermogenic capacity.

4. Discussion

Our results provide *in vivo* evidence that endogenous VEGF-A signaling in brown adipocytes occurs in an autocrine manner and is essential for BAT function. Our results also identify the adipocyte precursor cell population within WAT and BAT as the cell type expressing the highest levels of VEGF-A, with higher expression in the population from BAT compared to WAT. We show that ablation of endogenous VEGF-A specifically in adipose tissue results in mice that display decreased vascularity and disrupted lipid architecture in BAT. These observations are functionally relevant in that these mice are unable to respond to cold, indicating a dependence on VEGF-A signaling to facilitate the thermogenic response. In contrast, we do not observe any changes to these parameters in mice lacking VEGF-A specifically in macrophages. Assessment of mitochondria revealed reduced mass and size, which had functional consequences as evidenced by decreased oxygen consumption rates in mice lacking VEGF-A in adipose tissue. Interestingly, acute VEGF-A ablation resulted in reduced mitochondrial respiration in response to NE, without significant changes in maximal oxidative capacity or mitochondrial mass.

Several publications underscore the significance of adipose tissue angiogenesis and therapeutic potential for obesity-related inflammation and complications. It has been demonstrated that VEGF-A, while critical for angiogenesis, is also crucial to the induction of beige adipocytes in white adipose tissue, suggesting that adipose tissue expansion in conditions such as obesity could benefit by targeting VEGF-A (32). Two publications using gain-of-function mouse models engineered to overexpress VEGF-A demonstrated increased adipose tissue vascularization and protection against systemic metabolic dysfunction (as induced by high fat diet) (33,34). Another recently published study employs overexpression of VEGF-A in BAT to demonstrate increased thermogenesis and improvement of glucose metabolism (35). However, these overexpression studies did not address the role of endogenous VEGF, as we have shown here.

Many cell types are affected by VEGF in a paracrine manner, although few instances of autocrine effects have been described. A decade of evidence demonstrates autocrine signaling of VEGF in the renal podocyte within the kidney (36-38). Furthermore, studies in mice and humans suggest that diabetic glomerular disease may partially be due to autocrine VEGF activity (39,40). In addition, the recent study of cardiac myocyte-derived VEGF revealed that autocrine signaling results in increased fatty acid delivery to the heart (41). Furthermore, while deletion of VEGF in adipose tissue results in increased WAT inflammation, increased lipid accumulation in BAT, and impaired glucose tolerance (3,4), the contribution of other cell types expressing VEGF-A within BAT tissue was not explored, nor were the functional consequences of VEGF-A ablation on mitochondrial biogenesis. Bagchi et al. has shown histological evidence that VEGF neutralization results in decreased vascular density and structural changes to BAT mitochondria; however this was accomplished by systemic neutralization of VEGF by adenovirus, and data are limited to morphological changes in BAT (11). Using specific ablation of VEGF in adipose tissue, and in brown adipocytes *in vitro*, we demonstrate that the morphological changes to BAT observed with VEGF ablation have functional consequences on thermogenesis, due to direct autocrine effects.

While the capacity of the angiogenic signal by VEGF-A to drive BAT development has been shown (35), in the current manuscript, we demonstrate that this driving force is generated by BAT itself, suggesting that the angiogenic signal functions as a mechanism to induce both the thermogenic machinery utilizing the fuel and the vascular system transporting the fuel and oxygen for utilization. This may serve to assure that thermogenic capacity cannot be developed unless the angiogenic signal is being produced. Consequences of uncoupling capacity in the absence of appropriate blood vessels could result in ischemia and further progression of disease.

In conclusion, our data demonstrate that VEGF-A expression by brown adipocytes provides a necessary autocrine signal to maintain mitochondrial oxidative capacity within the BAT. Disrupted angiogenic signaling in adipose tissue results in a functional impairment of BAT thermogenesis due, in part, to reduced mitochondrial respiration. Our understanding of the function and signaling pathway of VEGF-A in brown adipocytes will allow for future research to provide new therapeutic approaches to the treatment of obesity and obesity-related cardiovascular disease.

Supplementary Material

Refer to Web version on PubMed Central for supplementary material.

Acknowledgements

We thank Susan Fried for helpful discussion. We thank Raffi Gharakhanian, Shi Su, Zachary Weitzner, and Maria A. Zuriaga for technical help. The $VEGF^{flox/flox}$ mouse was provided by Genentech (MTA: OM-213542).

Funding. The project described was supported by K01 AR055965-02 grant from NIAMS/NIH to T.A.; Pilot and Feasibility Grant P30 DK046200 from the Boston Nutrition Obesity Research Center to T.A.; and National Institutes of Health UL1RR025771 from the Clinical and Translational Science Institute at Boston University to T.A. Its contents are solely the responsibility of the author and do not necessarily represent the official views of the NIAMS or NIH.

List of Abbreviations

BAT	brown adipose tissue
NE	norepinephrine
OCR	oxygen consumption rate
VEGF-A	vascular endothelial growth factor-A
WAT	white adipose tissue

References

1. Ye J, Gao Z, Yin J, He Q. Hypoxia is a potential risk factor for chronic inflammation and adiponectin reduction in adipose tissue of ob/ob and dietary obese mice. Am J Physiol Endocrinol Metab. 2007; 293:E1118–1128. [PubMed: 17666485]
2. Lijnen HR, Christiaens V, Scroyen I, Voros G, Tjwa M, Carmeliet P, Collen D. Impaired adipose tissue development in mice with inactivation of placental growth factor function. Diabetes. 2006; 55:2698–2704. [PubMed: 17003333]
3. Shimizu I, Aprahamian T, Kikuchi R, Shimizu A, Papanicolaou KN, Maclauchlan S, Maruyama S, Walsh K. Vascular rarefaction mediates whitening of brown fat in obesity. J Clin Invest. 2014; 124:2099–2112. [PubMed: 24713652]
4. Sung HK, Doh KO, Son JE, Park JG, Bae Y, Choi S, Nelson SM, Cowling R, Nagy K, Michael IP, Koh GY, Adamson SL, Pawson T, Nagy A. Adipose vascular endothelial growth factor regulates metabolic homeostasis through angiogenesis. Cell Metab. 2013; 17:61–72. [PubMed: 23312284]
5. Nedergaard J, Bengtsson T, Cannon B. Three years with adult human brown adipose tissue. Ann N Y Acad Sci. 2010; 1212:E20–36. [PubMed: 21375707]
6. Yoneshiro T, Aita S, Matsushita M, Okamatsu-Ogura Y, Kameya T, Kawai Y, Miyagawa M, Tsujisaki M, Saito M. Age-related decrease in cold- activated brown adipose tissue and accumulation of body fat in healthy humans. Obesity (Silver Spring). 2011; 19:1755–1760. [PubMed: 21566561]
7. Hagberg CE, Falkevall A, Wang X, Larsson E, Huusko J, Nilsson I, van Meeteren LA, Samen E, Lu L, Vanwildemeersch M, Klar J, Genove G, Pietras K, Stone-Elander S, Claesson-Welsh L, Yla-Herttuala S, Lindahl P, Eriksson U. Vascular endothelial growth factor B controls endothelial fatty acid uptake. Nature. 2010; 464:917–921. [PubMed: 20228789]
8. Fredriksson JM, Nikami H, Nedergaard J. Cold-induced expression of the VEGF gene in brown adipose tissue is independent of thermogenic oxygen consumption. FEBS Lett. 2005; 579:5680–5684. [PubMed: 16219308]
9. Bartelt A, Bruns OT, Reimer R, Hohenberg H, Ittrich H, Peldschus K, Kaul MG, Tromsdorf UI, Weller H, Waurisch C, Eychmuller A, Gordts PL, Rinninger F, Bruegelmann K, Freund B, Nielsen

P, Merkel M, Heeren J. Brown adipose tissue activity controls triglyceride clearance. Nat Med. 2011; 17:200–205. [PubMed: 21258337]

10. Xue Y, Petrovic N, Cao R, Larsson O, Lim S, Chen S, Feldmann HM, Liang Z, Zhu Z, Nedergaard J, Cannon B, Cao Y. Hypoxia-independent angiogenesis in adipose tissues during cold acclimation. Cell Metab. 2009; 9:99–109. [PubMed: 19117550]
11. Bagchi M, Kim LA, Boucher J, Walshe TE, Kahn CR, D'Amore PA. Vascular endothelial growth factor is important for brown adipose tissue development and maintenance. FASEB J. 2013; 27:3257–3271. [PubMed: 23682123]
12. Hovey RC, Goldhar AS, Baffi J, Vonderhaar BK. Transcriptional regulation of vascular endothelial growth factor expression in epithelial and stromal cells during mouse mammary gland development. Mol Endocrinol. 2001; 15:819–831. [PubMed: 11328861]
13. Saint-Geniez M, Maharaj AS, Walshe TE, Tucker BA, Sekiyama E, Kurihara T, Darland DC, Young MJ, D'Amore PA. Endogenous VEGF is required for visual function: evidence for a survival role on muller cells and photoreceptors. PLoS One. 2008; 3:e3554. [PubMed: 18978936]
14. Guan F, Villegas G, Teichman J, Mundel P, Tufro A. Autocrine VEGF-A system in podocytes regulates podocin and its interaction with CD2AP. Am J Physiol Renal Physiol. 2006; 291:F422–428. [PubMed: 16597608]
15. Rodbell M. Metabolism of Isolated Fat Cells. I. Effects of Hormones on Glucose Metabolism and Lipolysis. J Biol Chem. 1964; 239:375–380. [PubMed: 14169133]
16. Rodeheffer MS, Birsoy K, Friedman JM. Identification of white adipocyte progenitor cells in vivo. Cell. 2008; 135:240–249. [PubMed: 18835024]
17. Nishimura S, Manabe I, Nagasaki M, Hosoya Y, Yamashita H, Fujita H, Ohsugi M, Tobe K, Kadowaki T, Nagai R, Sugiura S. Adipogenesis in obesity requires close interplay between differentiating adipocytes, stromal cells, and blood vessels. Diabetes. 2007; 56:1517–1526. [PubMed: 17389330]
18. Wikstrom JD, Mahdaviani K, Liesa M, Sereda SB, Si Y, Las G, Twig G, Petrovic N, Zingaretti C, Graham A, Cinti S, Corkey BE, Cannon B, Nedergaard J, Shirihai OS. Hormone-induced mitochondrial fission is utilized by brown adipocytes as an amplification pathway for energy expenditure. EMBO J. 2014; 33:418–436. [PubMed: 24431221]
19. Cannon B, Nedergaard J. Cultures of adipose precursor cells from brown adipose tissue and of clonal brown-adipocyte-like cell lines. Methods Mol Biol. 2001; 155:213–224. [PubMed: 11293074]
20. Petrovic N, Walden TB, Shabalina IG, Timmons JA, Cannon B, Nedergaard J. Chronic peroxisome proliferator-activated receptor gamma (PPARgamma) activation of epididymally derived white adipocyte cultures reveals a population of thermogenically competent, UCP1-containing adipocytes molecularly distinct from classic brown adipocytes. J Biol Chem. 2010; 285:7153–7164. [PubMed: 20028987]
21. Wu M, Neilson A, Swift AL, Moran R, Tamagnine J, Parslow D, Armistead S, Lemire K, Orrell J, Teich J, Chomicz S, Ferrick DA. Multiparameter metabolic analysis reveals a close link between attenuated mitochondrial bioenergetic function and enhanced glycolysis dependency in human tumor cells. Am J Physiol Cell Physiol. 2007; 292:C125–136. [PubMed: 16971499]
22. Ahmadian M, Abbott MJ, Tang T, Hudak CS, Kim Y, Bruss M, Hellerstein MK, Lee HY, Samuel VT, Shulman GI, Wang Y, Duncan RE, Kang C, Sul HS. Desnutrin/ATGL is regulated by AMPK and is required for a brown adipose phenotype. Cell Metab. 2011; 13:739–748. [PubMed: 21641555]
23. Batra A, Okur B, Glauben R, Erben U, Ihbe J, Stroh T, Fedke I, Chang HD, Zeitz M, Siegmund B. Leptin: a critical regulator of CD4+ T-cell polarization in vitro and in vivo. Endocrinology. 2010; 151:56–62. [PubMed: 19966187]
24. Cybulski N, Polak P, Auwerx J, Ruegg MA, Hall MN. mTOR complex 2 in adipose tissue negatively controls whole-body growth. Proc Natl Acad Sci U S A. 2009; 106:9902–9907. [PubMed: 19497867]
25. Li P, Fan W, Xu J, Lu M, Yamamoto H, Auwerx J, Sears DD, Talukdar S, Oh D, Chen A, Bandyopadhyay G, Scadeng M, Ofrecio JM, Nalbandian S, Olefsky JM. Adipocyte NCoR

knockout decreases PPARgamma phosphorylation and enhances PPARgamma activity and insulin sensitivity. Cell. 2011; 147:815–826. [PubMed: 22078880]

26. Minamino T, Orimo M, Shimizu I, Kunieda T, Yokoyama M, Ito T, Nojima A, Nabetani A, Oike Y, Matsubara H, Ishikawa F, Komuro I. A crucial role for adipose tissue p53 in the regulation of insulin resistance. Nat Med. 2009; 15:1082–1087. [PubMed: 19718037]
27. Polak P, Cybulski N, Feige JN, Auwerx J, Ruegg MA, Hall MN. Adipose-specific knockout of raptor results in lean mice with enhanced mitochondrial respiration. Cell Metab. 2008; 8:399–410. [PubMed: 19046571]
28. Wueest S, Rapold RA, Schumann DM, Rytka JM, Schildknecht A, Nov O, Chervonsky AV, Rudich A, Schoenle EJ, Donath MY, Konrad D. Deletion of Fas in adipocytes relieves adipose tissue inflammation and hepatic manifestations of obesity in mice. J Clin Invest. 2010; 120:191–202. [PubMed: 19955656]
29. Jonker JW, Suh JM, Atkins AR, Ahmadian M, Li P, Whyte J, He M, Juguilon H, Yin YQ, Phillips CT, Yu RT, Olefsky JM, Henry RR, Downes M, Evans RM. A PPARgamma-FGF1 axis is required for adaptive adipose remodelling and metabolic homeostasis. Nature. 2012; 485:391–394. [PubMed: 22522926]
30. Cramer T, Yamanishi Y, Clausen BE, Forster I, Pawlinski R, Mackman N, Haase VH, Jaenisch R, Corr M, Nizet V, Firestein GS, Gerber HP, Ferrara N, Johnson RS. HIF-1alpha is essential for myeloid cell-mediated inflammation. Cell. 2003; 112:645–657. [PubMed: 12628185]
31. Peyssonnaux C, Cejudo-Martin P, Doedens A, Zinkernagel AS, Johnson RS, Nizet V. Cutting edge: Essential role of hypoxia inducible factor-1alpha in development of lipopolysaccharide-induced sepsis. J Immunol. 2007; 178:7516–7519. [PubMed: 17548584]
32. During MJ, Liu X, Huang W, Magee D, Slater A, McMurphy T, Wang C, Cao L. Adipose VEGF Links the White-to-Brown Fat Switch With Environmental, Genetic, and Pharmacological Stimuli in Male Mice. Endocrinology. 2015; 156:2059–2073. [PubMed: 25763639]
33. Sun K, Wernstedt Asterholm I, Kusminski CM, Bueno A, Wang Z, Pollard J, Brekken RA, Scherer PE. Dichotomous effects of VEGF-A on adipose tissue dysfunction. Proc Natl Acad Sci U S A. 2012; 109:5874–5879. [PubMed: 22451920]
34. Elias I, Franckhauser S, Ferre T, Vila L, Tafuro S, Munoz S, Roca C, Ramos D, Pujol A, Riu E, Ruberte J, Bosch F. Adipose tissue overexpression of vascular endothelial growth factor protects against diet-induced obesity and insulin resistance. Diabetes. 2012; 61:1801–1813. [PubMed: 22522611]
35. Sun K, Kusminski CM, Luby-Phelps K, Spurgin SB, An WA, Wang QA, Holland WL, Scherer PE. Brown adipose tissue derived VEGF-A modulates cold tolerance and energy expenditure. Molecular Metabolism. 2014; 3:474–483. [PubMed: 24944907]
36. Chen S, Kasama Y, Lee JS, Jim B, Marin M, Ziyadeh FN. Podocyte-derived vascular endothelial growth factor mediates the stimulation of alpha3(IV) collagen production by transforming growth factor-beta1 in mouse podocytes. Diabetes. 2004; 53:2939–2949. [PubMed: 15504975]
37. Foster RR, Hole R, Anderson K, Satchell SC, Coward RJ, Mathieson PW, Gillatt DA, Saleem MA, Bates DO, Harper SJ. Functional evidence that vascular endothelial growth factor may act as an autocrine factor on human podocytes. Am J Physiol Renal Physiol. 2003; 284:F1263–1273. [PubMed: 12620928]
38. Guan F, Villegas G, Teichman J, Mundel P, Tufro A. Autocrine class 3 semaphorin system regulates slit diaphragm proteins and podocyte survival. Kidney Int. 2006; 69:1564–1569. [PubMed: 16541019]
39. Veron D, Reidy KJ, Bertuccio C, Teichman J, Villegas G, Jimenez J, Shen W, Kopp JB, Thomas DB, Tufro A. Overexpression of VEGF-A in podocytes of adult mice causes glomerular disease. Kidney Int. 2010; 77:989–999. [PubMed: 20375978]
40. Hohenstein B, Colin M, Foellmer C, Amann KU, Brekken RA, Daniel C, Hugo CP. Autocrine VEGF-VEGF-R loop on podocytes during glomerulonephritis in humans. Nephrol Dial Transplant. 2010; 25:3170–3180. [PubMed: 20395257]
41. Zhang D, Wan A, Chiu AP, Wang Y, Wang F, Neumaier K, Lal N, Bround MJ, Johnson JD, Vlodavsky I, Rodrigues B. Hyperglycemia-induced secretion of endothelial heparanase stimulates a vascular endothelial growth factor autocrine network in cardiomyocytes that promotes

recruitment of lipoprotein lipase. Arterioscler Thromb Vasc Biol. 2013; 33:2830–2838. [PubMed: 24115032]

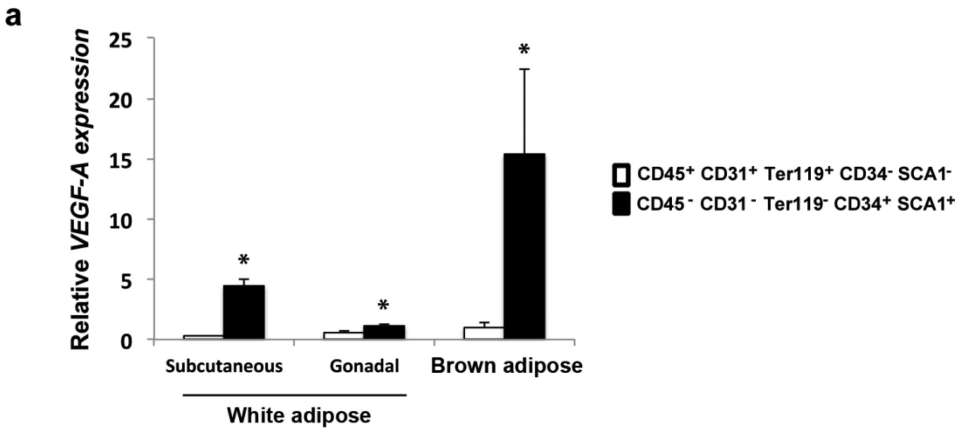

Figure 1.

VEGF-A expression in sorted SVF cell populations from WAT and BAT. Expression levels of VEGF-A were measured by qRT-PCR in lineage specific cell populations, representing hematopoietic and myeloid progenitors ($CD45^+$ $CD31^+$ $Ter119^+$ $CD34^-$ $SCA1^-$), as well as adipocyte precursors ($CD45^-$ $CD31^-$ $Ter119^-$ $CD34^+$ $SCA1^+$). Stromal vascular cells were isolated and sorted from WAT and BAT from male wild type mice. Results are representative of 3 separate experiments pooling three mice each for WAT, and two mice each for BAT. Data are means ± SEM. *p <0.05 compared to $CD45^+$ $CD31^+$ $Ter119^+$ $CD34^-$ $SCA1^-$ cells.

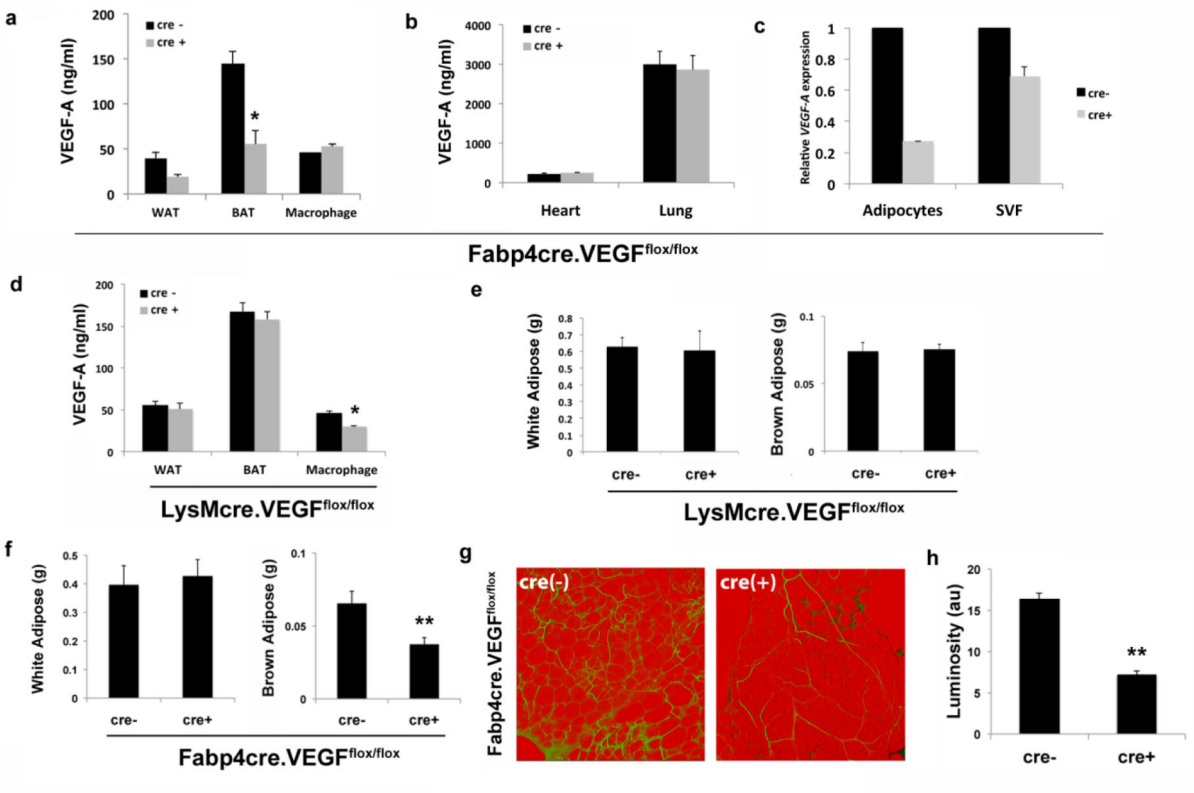

Figure 2.

Tissue-specific ablation of VEGF-A. VEGF-A protein expression in a) WAT, BAT, macrophages, b) heart and lung from Fabp4-cre(−).VEGF$^{flox/flox}$ and Fabp4-cre(+).VEGF$^{flox/flox}$ mice quantified by ELISA. c) mRNA expression levels of VEGF-A in adipocyte and stromal vascular fraction (SVF) from BAT of Fabp4-cre(−).VEGF$^{flox/flox}$ and Fabp4-cre(+).VEGF$^{flox/flox}$ mice. d) VEGF-A protein expression in WAT, BAT, and peritoneal macrophages from LysM-cre(−).VEGF$^{flox/flox}$ and LysM-cre(+).VEGF$^{flox/flox}$ mice quantified by ELISA. e) Epididymal fat pad (WAT) and interscapular brown adipose (BAT) weights were measured in male LysM-cre(−).VEGF$^{flox/flox}$ and LysM-cre(+).VEGF$^{flox/flox}$ mice. f) Epididymal fat pad (WAT) and interscapular brown adipose (BAT) weights were measured in male Fabp4-cre(−).VEGF$^{flox/flox}$ and Fabp4-cre(+).VEGF$^{flox/flox}$ mice. g) Representative confocal micrographs and h) quantification of vascularization in epididymal fat pads stained with BS1-lectin (FITC) for vasculature and BODIPY (Texas Red) for adipocytes. Vascularity is expressed as arbitrary units of luminosity (au). (Fabp4Cre(−) mice, n=15; Fabp4Cre(+) mice, n=13; LysMcre (−) mice, n=11; LysMcre (+) mice, n=13;). *p <0.01; **p <0.002

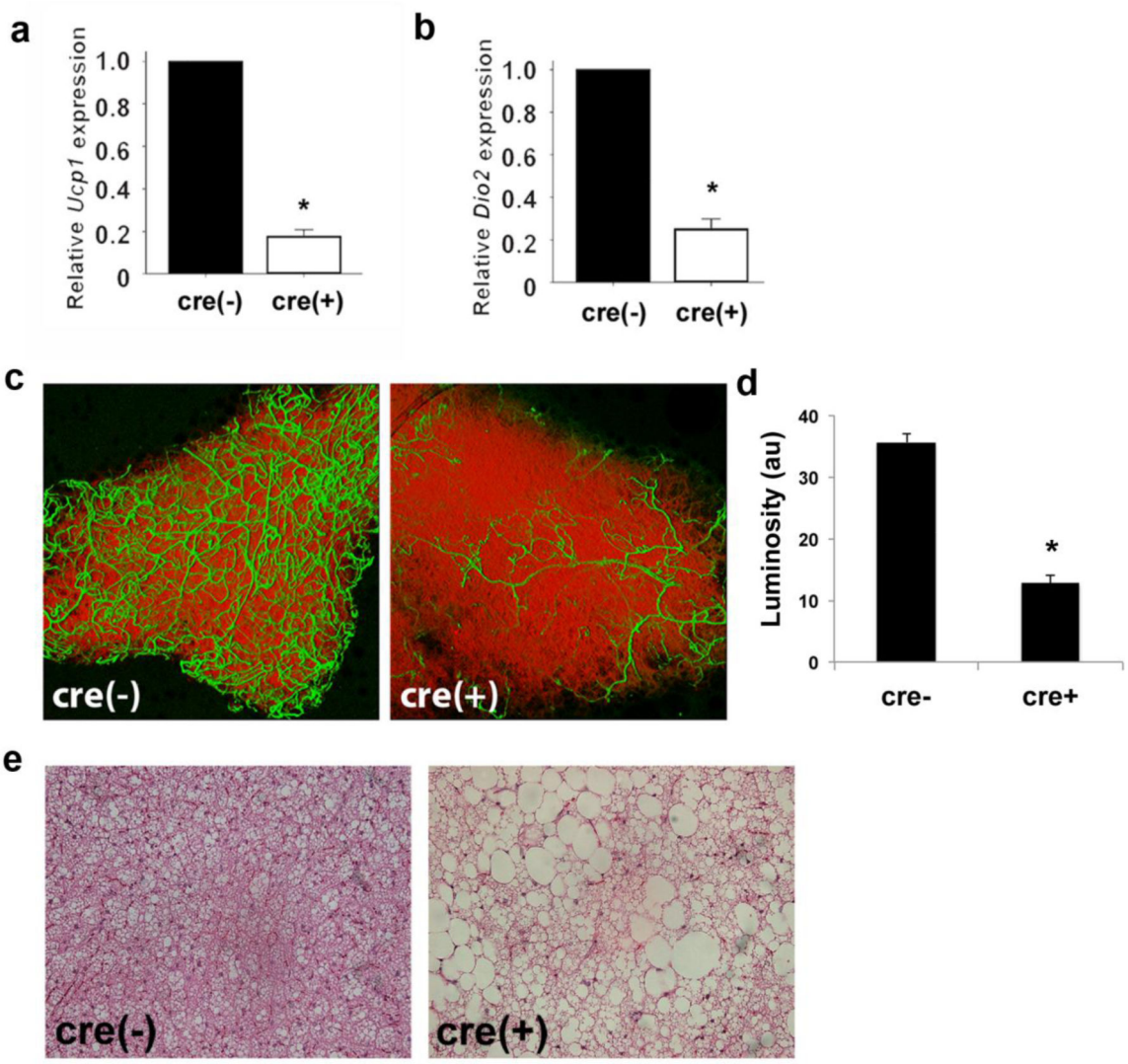

Figure 3.

Disrupted BAT phenotype in mice with adipose-specific VEGF-A ablation. Expression of BAT markers, a) Ucp1 and b) Dio2, was assessed by qRT-PCR. c) VEGF-A ablation results in decreased vascularization in BAT as visualized with BS1-lectin (FITC) for vasculature and BODIPY (Texas Red) for adipocytes. d) Quantification of vascularity expressed as arbitrary units of luminosity (au). e) Disruption of lipid architecture in BAT shown by representative hematoxylin and eosin staining. *p <0.01; **p <0.05

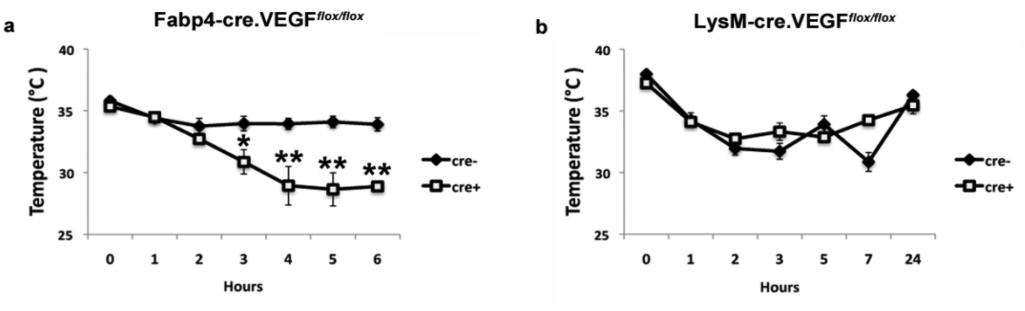

Figure 4.

Impaired tolerance to cold in Fabp4cre(+).VEGF$^{flox/flox}$ mice. a) 8-12 week old mice were placed at 4°. Temperatures were measured hourly for 6 hours, using implanted microchip transponders. Cre(−) (n=19) cre(+) (n=19). b) LysMcre(+).VEGF$^{flox/flox}$ (n=13) and LysMcre(−).VEGF$^{flox/flox}$ mice (n=11) were subjected to cold tolerance testing for 24 hours. *p <0.01; **p <0.001

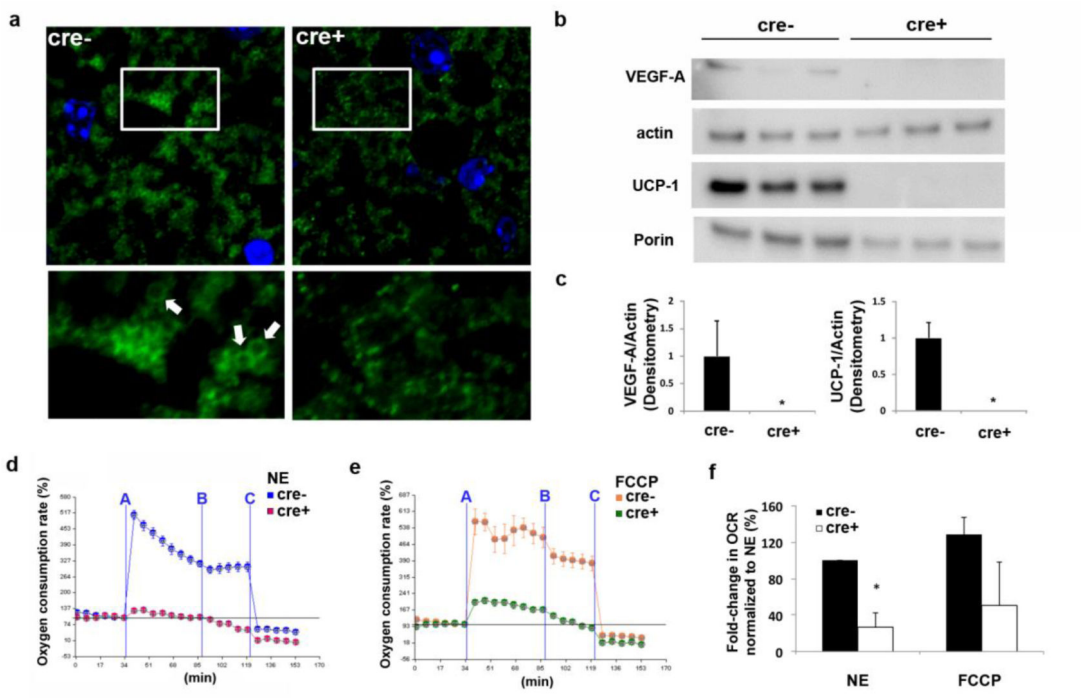

Figure 5.

Complete ablation of VEGF-A in brown adipocytes disrupts mitochondrial structure and impairs mitochondrial respiration. a) Representative images of formalin fixed BAT from Fabp4cre(−).VEGF$^{flox/flox}$ and Fabp4cre(+).VEGF$^{flox/flox}$ mice stained with Tomm20. Ring-shaped mitochondria are observed only in Fabp4cre(−).VEGF$^{flox/flox}$ mice (arrows) b) Western blotting was performed on isolated brown adipocytes from Fabp4cre(−).VEGF$^{flox/flox}$ and Fabp4cre(+).VEGF$^{flox/flox}$ mice for VEGF-A, actin, UCP-1, and porin, and c) quantified. After treatment with d) norepinephrine (NE) or e) FCCP + sodium pyruvate, the oxygen consumption rate of mitochondria from VEGF-sufficient or -deficient brown adipocytes was examined by Seahorse extracellular flux analyzer and f) quantified. Timepoints of stimulation/inhibition (blue lines) A=NE(1 μM) or FCCP(5 μM) + sodium pyruvate (10 mM); B=Oligomycin (5 μM); and C=Antimycin(8 μM). Experiments were run in triplicate and data were combined in order to perform statistics. ** p<0.005

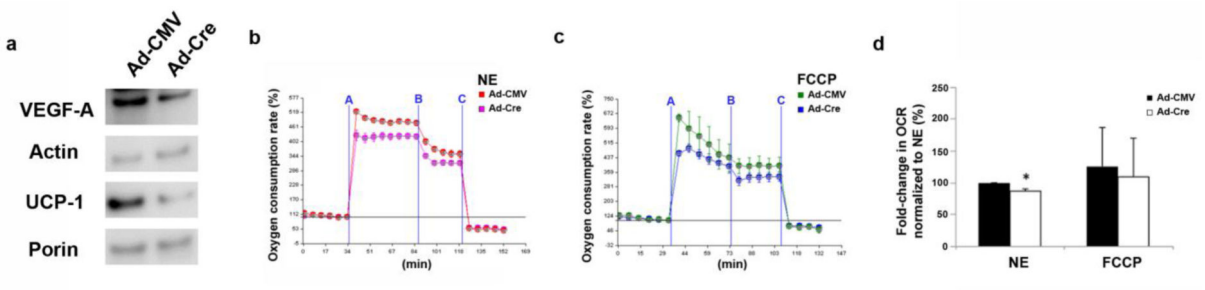

Figure 6.

Acute ablation of VEGF-A in brown adipocytes impairs mitochondrial respiration. Brown adipocytes were isolated from VEGF$^{flox/flox}$ mice, and treated with adeno-CMV control (Ad-CMV) virus or adeno-Cre recombinase (Ad-Cre). a) Western blotting was performed for VEGF-A, actin, UCP-1, and porin on isolated brown adipocytes from VEGF$^{flox/flox}$ mice isolated treated with Ad-CMV or Ad-Cre at day 4 of differentiation. After treatment with b) NE or c) FCCP + sodium pyruvate, the oxygen consumption rate of mitochondria from VEGF$^{flox/flox}$ brown adipocytes treated with Ad-Cre or Ad-CMV was examined by Seahorse extracellular flux analyzer and d) quantified. Timepoints of stimulation/inhibition (blue lines) A=NE(1 μM) or FCCP (5 μM) + sodium pyruvate (10 mM); B=Oligomycin (5 μM); and C=Antimycin (8 μM). Experiments were run in separate attempts (n=4) and data were combined in order to perform statistics. *p<0.05